Role of microRNA-21 in hypertrophic cardiac remodeling

Ken Watanabe[1], Taro Narumi[*2], Tetsu Watanabe[1], Yoichiro Otaki[3], Tetsuya Takahashi[1], Tomonori Aono[1], Jun Goto[1], Taku Toshima[1], Takayuki Sugai[1], Masahiro Wanezaki[1], Daisuke Kutsuzawa[4], Shigehiko Kato[1], Harutoshi Tamura[1], Satoshi Nishiyama[1], Hiroki Takahashi[3], Takanori Arimoto[1], Tetsuro Shishido[1], Masafumi Watanabe[1, 3, 4]

[1] Department of Cardiology, Pulmonology, and Nephrology, Yamagata University School of Medicine, Yamagata, Japan.

[2] Department of Cardiology, Internal Medicine III, Hamamatsu University School of Medicine, Hamamatsu, Japan.

[3] Department of Advanced Cardiovascular Therapeutics, Yamagata University School of Medicine, Yamagata, Japan.

[4] Department of Advanced Heart Rhythm Therapeutics, Yamagata University School of Medicine, Yamagata, Japan.

***Address for correspondence:** Taro Narumi, MD, PhD
E-mail: ajitaro910@gmail.com (TN)

Abstract

Hypertension is a major public health problem among with aging population worldwide. It causes cardiac remodeling, including hypertrophy and interstitial fibrosis, which leads to development of hypertensive heart disease (HHD). Although microRNA-21 (miR-21) is associated with fibrogenesis in multiple organs, its impact on hypertrophic cardiac remodeling in hypertension is not known. Circulating miR-21 level was higher in patients with HHD than that in the control subjects. It also positively correlated with serum myocardial fibrotic markers. MiR-21 expression levels were significantly upregulated in the mice hearts after angiotensin II (Ang II) infusion or transverse aortic constriction (TAC) compared with control mice. Expression level of programmed cell death 4 (PDCD4), a main target of miR-21, was significantly decreased in Ang II infused mice and TAC mice compared with control mice. Expression levels of transcriptional activator protein 1 (AP-1) and transforming growth factor-β1 (TGF-β1), which were downstream targets of PDCD4, were increased in Ang II infused mice and TAC mice compared with control mice. *In vitro*, mirVana-miR-21-specific inhibitor attenuated Ang II-induced PDCD4 downregulation and contributed to subsequent deactivation of AP-1/TGF-β1 signaling pathway in neonatal rat cardiomyocytes. Thus, suppression of miR-21 prevents hypertrophic cardiac remodeling by regulating PDCD4,

AP-1, and TGF-β1 signaling pathway.

Introduction

Hypertension is a major public health concern among the elderly population worldwide. It is associated with increased risk of adverse cardiovascular events [1]. An epidemiological report indicated that 31.1 % of adults in the world (1.39 billion people) had hypertension in 2010 [2]. Hypertension increases the risk of developing hypertension-induced organ damages, such as hypertensive heart disease (HHD), hypertensive encephalopathy, and nephrosclerosis [3]. HHD is one of the most important hypertension-induced organ damages [4]. According to the Framingham Heart Study, 20 mmHg increase in systolic blood pressure contributes to 56% increased risk for heart failure [5]. Furthermore, it was reported that HHD is a common pathophysiology of heart failure with preserved ejection fraction [6, 7]. Hypertension causes cardiac remodeling characterized by cardiac fibrosis, which contributes to progression of heart failure [3, 4].

MicroRNAs (miRs) are small non-coding RNAs that regulate post-transcriptional gene expressions. They have been shown to play an important role in fibrogenic process in multiple organs [8]. In the present study, we focused on the fibrogenic function of miR-21, which is a ubiquitously expressed miR that is reported to have a pivotal role in development of tissue fibrosis [9]. Transforming growth factor-β1 (TGF-β1), a

57 pleiotropic and multifactorial cytokine involved in many biological processes, plays a
58 crucial role in the pathogenesis of cardiac remodeling in hypertension [10]. It has been
59 demonstrated that miR-21 can promote TGF-β1 signaling [11, 12]. On the other hand,
60 miR-21 has been found to be upregulated by TGF-β1 [13]. This interrelationship forms
61 a positive feedback loop, which may exacerbate the fibrogenic process. Previous studies
62 have also demonstrated the contribution of miR-21 in patients with aortic stenosis,
63 hypertrophic cardiomyopathy, and dilated cardiomyopathy [14-16]. However, the
64 impact of miR-21 on the pathogenesis of hypertrophic cardiac remodeling in
65 hypertension is still not clear.

66 We hypothesized that miR-21 deteriorates hypertrophic cardiac remodeling by
67 enhancing TGF-β1 signaling pathway through suppressing its target gene expression. In
68 the present study, we investigated the following: (1) miR-21 expression levels in
69 patients with HHD; (2) miR-21 expression levels and its downstream signaling in
70 animal model of hypertrophic cardiac remodeling by transverse aortic constriction
71 (TAC) or angiotensin II (Ang II) infusion; (3) the function of miR-21 in cardiac
72 remodeling process in response to Ang II stimulation *in vitro*; (4) the therapeutic
73 potential of miR-21 inhibitor in hypertrophic cardiac remodeling *in vitro*.

Materials and Methods

Human studies

The present study included 10 patients with HHD and 10 control patients who were assessed to rule out cardiomyopathy and heart failure, and had normal cardiac function (Table 1). Endomyocardial biopsies (EMBs) were collected from the patients who had left ventricular hypertrophy and suspected some types of cardiomyopathy. EMBs were taken from left ventricle with a total of 4 to 6 samples through the femoral arteries. EMBs were analyzed in 3 HHD patients who were excluded other cardiomyopathy based on EMBs and other clinical data, and 3 control patients who had transient left ventricular dysfunction and suspected myocarditis but were eventually ruled out cardiomyopathy. The final diagnosis of HHD were made by two expert cardiologists based on angiography, echocardiographic data, clinical background, and medical history. Written informed consent was obtained from all patients before the study. The protocol was performed in accordance to the Helsinki Declaration and was approved by the human investigations committee of Yamagata University School of Medicine.

Table 1. Clinical characteristics of 10 control subjects and 10 HHD patients.

Variables	Control patients $n = 10$	HHD patients $n = 10$	*P* value
Age (years old)	61 ± 8	58 ± 12	ns
Male / Female	6 / 4	7 / 3	ns
BMI (kg/m^2)	23.7 ± 1.9	26.1 ± 5.9	ns
Hypertension, n (%)	3 (30)	10 (100)	<0.05
Diabetes mellitus, n (%)	1 (10)	6 (60)	<0.05
Dyslipidemia, n (%)	3 (30)	4 (40)	ns
NYHA functional class III-IV, n (%)	0 (0)	4 (40)	<0.05
Echocardiographic data			
LVEDD (mm)	47 ± 5	55 ± 9	<0.05
LVEF (%)	68 ± 6	52 ± 14	<0.05
IVSD (mm)	9 ± 2	14 ± 2	<0.05
LVPWD (mm)	10 ± 1	13 ± 2	<0.05
Blood examination			
eGFR (mL/min/1.73 m^2)	92.0 ± 18.9	56.3 ± 25.5	<0.05
BNP (pg/mL)	36 (17 - 70)	463 (143 - 713)	<0.05
Medications			
ACEIs and/or ARBs, n (%)	3 (30)	10 (100)	<0.05
CCBs, n (%)	1 (10)	7 (70)	<0.05
Diuretics, n (%)	0 (0)	6 (60)	<0.05
Statins, n (%)	3 (30)	5 (50)	ns

Data are expressed as mean ± SD, number (percentage), or median (interquartile range). ACEIs, angiotensin-converting enzyme inhibitors; ARBs, angiotensin II receptor blockers; BMI, body mass index; BNP, B-type natriuretic peptide; CCBs, calcium-channel blockers; eGFR, estimated glomerular filtration rate; HHD, hypertensive heart disease; IVSD, interventricular septum diameter; LVEDD, left ventricular end-diastolic diameter; LVEF, left ventricular ejection fraction; LVPWD, left ventricular posterior wall diameter; NYHA, New York Heart Association.

Measurement of circulating miR-21 levels and biochemical assays

Blood samples were collected in the early morning within 24 hours after admission, centrifuged at 3000g for 15 min at 4 ℃, and the obtained serum was stored at −80 ℃. Circulating miRs were isolated from 300 μL serum by using a NucleoSpin microRNA isolation kit (TaKaRa, Otsu, Japan).

Serum carboxy-terminal telopeptide of type I collagen (I-CTP) concentrations were determined by radioimmunoassay (Orion Diagnostica, Finland) [17]. Serum procollagen type III N-terminal propeptide (P3NP) levels were measured with enzyme-linked immunosorbent assay (ELISA) kit (MyBioSource, San Diego, CA, USA).

Animal treatment regimens

Hypertension-induced cardiac remodeling models were established by Ang II infusions or TAC surgery [18, 19]. Briefly, Ang II was infused with ALZET osmotic pumps (1.5 mg/kg/day) as we previously described [18]. Cardiac function, dimension, and blood pressure were assessed after 2 weeks from Ang II infusion. The mice were sacrificed by intraperitoneal injection of a combination of ketamine (1g/kg) and xylazine (100 mg/kg), and the heart samples were obtained for the biochemical and histopathological

study. TAC surgery was performed to induce chronic pressure overload as we previously described [20]. Briefly, 8- to 10-week-old mice were anesthetized by intraperitoneal injection with a mixture of ketamine (80 mg/kg) and xylazine (8 mg/kg). Animals were intubated and ventilated with a rodent ventilator (Harvard Apparatus, Holliston, MA, USA). The transverse aortic arch was ligated (7-0 prolene) between the right innominate and left common carotid arteries with a 27-gauge needle, and then the needle was promptly removed leaving a discrete region of stenosis. Cardiac remodeling was assessed after 4 weeks from surgery. All experimental procedures were performed according to the animal welfare regulations of Yamagata University School of Medicine, and the study protocol was approved by the Animal Subjects Committee of Yamagata University School of Medicine. The investigation conformed to the Guide for the Care and Use of Laboratory Animals published by the US National Institutes of Health (NIH Publication, 8th Edition, 2011).

Neonatal rat cardiomyocyte isolation, cell culture, and treatment

Isolation and culture of neonatal rat cardiomyocytes (NRCMs) were performed as we previously described [21]. Briefly, ventricles were obtained from 1- to 2-day-old

133 Sprague-Dawley rat pups after euthanasia by decapitation, and cardiomyocytes were
134 isolated by digestion with collagenase. Cardiomyocytes were kept in serum-
135 supplemented (10% fatal bovine serum, FBS) Dulbecco's Modified Eagle Medium
136 (DMEM, Thermo Fisher Scientific, MA, USA). Primary culture of cardiofibroblasts
137 were obtained as previously described [22]. Briefly, ventricles of Sprague-Dawley rat
138 pups were digested with collagenase, and resuspended in DMEM with 10% FBS. Cells
139 were then seeded into 10-cm culture dishes and cultured at 37 ℃ for 2h. Unattached
140 cells were discarded, and attached cells were cultured in DMEM with 10% FBS.
141 NRCMs were transfected with small interfering RNA (siRNA) specific for programmed
142 cell death 4 (PDCD4) (Thermo Fisher Scientific), 10-nM mirVana hsa-miR-21 specific
143 inhibitor (Thermo Fisher Scientific), or mirVana miRNA inhibitor Negative Control
144 (Thermo Fisher Scientific) using Lipofectamine 3000 Reagent (Thermo Fisher
145 Scientific) according to the manufacturer's instructions. The medium was replaced with
146 DMEM with 10% FBS after transfection for 4h. NRCMs were stimulated with 1 μM
147 Ang II for 24 hours of serum starvation.
148

149 # Western blotting

150 The total protein extracts were prepared with radio-immunoprecipitation assay (RIPA)

151 buffer as we previously reported [21]. Equal amounts of protein were subjected to 10%
152 SDS-PAGE and transferred to polyvinylidene difluoride membranes. The membranes
153 were probed overnight at 4 ℃ with the following primary antibodies: PDCD4 (Santa
154 Cruz, Dallas, TX, USA, sc-376430), c-Jun (Cell Signaling Technology, Danvers, MA,
155 USA, #9165), TGF-β1 (Cell Signaling Technology, #3711), phospho-transforming
156 growth factor-β-activated kinase 1 (p-TAK1) (Cell Signaling Technology, #4537),
157 TAK1 (Cell Signaling Technology, #4505), β-tubulin (Cell Signaling Technology,
158 #2146). Protein expression levels were normalized to that of β-tubulin.
159

160 RNA extraction and quantitative reverse transcription
161 polymerase chain reaction (qRT-PCR)

162 Total RNA was isolated from human endomyocardial biopsy specimens, mouse whole
163 heart, and NRCMs using TRIzol reagent (Thermo Fisher Scientific) as we previously
164 described [23]. For miRs screening assay, first strand cDNA of miRs was synthesized,
165 and PCR reaction was performed using a miR-X miRNA qRT-PCR SYBR Kit
166 (TaKaRa) according to the manufacturer's instructions. For other studies, first strand
167 cDNA was synthesized using a Superscript IV First-strand cDNA synthesis kit (Thermo
168 Fisher Scientific) and quantitative RT-PCR (qRT-PCR) was performed with SYBR

Green Real-Time PCR Master Mixes (Thermo Fisher Scientific) according to the manufacturer's instructions. Gene expressions was normalized to U6 for miR assay and β-actin for other assays.

Histopathological examinations

Biopsy samples of human cardiomyocyte and mice heart samples were fixed with 4% formalin and embedded in paraffin. Sections of 3–5 μm thickness were stained with hematoxylin-eosin (HE) or Massons's trichrome stain for histopathological analysis as we previously described [20]. The extent of myocardial interstitial fibrosis was evaluated using a microscope and attached software (BZ-X710; Keyence, Osaka, Japan).

Statistical analysis

All values are expressed as mean ± standard error of mean (SEM). Statistical differences among groups were evaluated with one-way analysis of variance (ANOVA) followed by Tukey-Kramer post hoc tests. Correlations between the circulating miRs levels and biomarkers of cardiac fibrosis were analyzed by using Pearson's correlation coefficient. A value of $P < 0.05$ was considered statistically significant. All statistical

187 analyses were performed with a standard software package (JMP version 12; SAS

188 institute, Cary, NC, USA).

Results

MiRs expression levels in patients with hypertensive heart disease

To investigate the expression levels of fibrosis-associated miRs according to previous report [24], we first measured the levels of circulating miR-21, miR-29, miR-30, and miR-133 in patients with HHD. Circulating miR-21 levels were significantly increased in patients with HHD compared with those of control subjects. On the other hand, circulating miR-29, miR-30, and miR-133 levels were significantly decreased in patients with HHD (Fig. 1A). HE and Masson's trichrome staining revealed that significant cardiac hypertrophy and fibrosis was observed in the heart section from patients with HHD (Fig. 1B). MiR-21 levels were significantly increased in the heart samples of patients with HHD compared with those of the normal subjects. In contrast, miR-29, miR-30, and miR-133 levels tended to be decreased in patients with HHD, but the differences were not statistically significant (Fig. 1C). We measured serum I-CTP and P3NP levels as markers of myocardial fibrosis [17, 25]. Serum I-CTP and P3NP levels were significantly higher in patients with HHD compared with those of control subjects (Fig. 1D). As shown in Fig. 1E, there were significant positive correlations between circulating miR-21 levels and serum I-CTP ($R = 0.560$) and P3NP ($R = 0.477$).

However, there were no significant correlations between other miRs and I-CTP (miR-29: R = −0.215; miR-30: R = −0.068; miR-133: R = 0.268) and P3NP (miR-29: R = −0.302; miR-30: R = −0.263; miR-133: R = −0.138) levels.

Fig 1. Association between miRs expressions and cardiac remodeling in patients with HHD.

(A) Circulating miRs expressions in patients with HHD (n = 10 per group). **(B)** Representative images and analysis of cardiac remodeling by HE and Masson's trichrome staining in heart samples from HHD patients and normal subjects (n = 3 per group). Scale bars = 20 μm. **(C)** Expression of miRs levels in heart samples from patients with HHD (n = 3 per group). **(D)** Serum I-CTP and P3NP levels in patients with HHD. **(E)** Circulating miR-21 levels were positively correlated with serum I-CTP and P3NP levels in patients with HHD. Data are expressed as mean ± SEM. **P* < 0.05, ***P* < 0.01.

MiR-21 expression levels in Ang II infused mice and TAC mice

MiR-21 expression levels were significantly increased in Ang II infused mice hearts

compared with those of sham mice (Fig. 2A). Cardiac remodeling was detected by HE and Masson's trichrome staining in Ang II infused mice hearts but not in sham mice (Fig. 2B). Alpha smooth muscle actin (α-SMA) mRNA expression was significantly upregulated in the Ang II infused mice hearts compared with those of the sham mice (Fig. 2C). Similarly, miR-21 expression levels were significantly increased in the heart of TAC mice compared with those of sham-operated mice (Fig. 2D). Cardiac remodeling was also detected by HE and Masson's trichrome staining in TAC mice but not in the sham-operated mice (Fig. 2E). α-SMA mRNA expression was significantly upregulated in the TAC mice hearts compared with those of the sham-operated mice (Fig. 2F). Echocardiographic and hemodynamic data of Ang II infused mice and TAC operated mice are shown in Table 2.

Fig 2. The crucial role of miR-21 in cardiac remodeling in Ang II infused and TAC mice models.

(A) MiR-21 expression levels in Ang II infused mice (n = 6 per group). **(B)** Representative images and analysis of cardiac remodeling by HE and Masson's trichrome staining in left ventricular sections in Ang II infused mice hearts (n = 6 per group). Scale bars = 50 μm. **(C)** α-SMA expression in Ang II infused mice (n = 6 per

group). **(D)** MiR-21 expression levels in the heart samples of TAC-operated mice (n = 6 per group). **(E)** Representative images and analysis of cardiac remodeling by HE and Masson's trichrome staining in left ventricular sections of the TAC-operated mice hearts (n = 6 per group). Scale bars = 50 μm. **(F)** α-SMA expression in TAC-operated mice (n = 6 per group). Data are expressed as mean ± SEM. $^{*}P < 0.05$, $^{**}P < 0.01$.

Table 2. Echocardiographic and hemodynamic data of Ang II infused mice and TAC operated mice.

	saline	Ang II	sham	TAC
LVEDD, mm	3.19 ± 0.11	2.96 ± 0.08	3.06 ± 0.16	3.13 ± 0.15
LVESD, mm	1.79 ± 0.11	1.58 ± 0.09	1.66 ± 0.16	2.45 ± 0.14†
IVSD, mm	0.76 ± 0.04	0.97 ± 0.03**	0.66 ± 0.03	0.99 ± 0.02†
LVPWD, mm	0.80 ± 0.03	0.94 ± 0.02**	0.72 ± 0.03	1.06 ± 0.03†
FS, %	45.9 ± 2.1	46.9 ± 1.6	45.6 ± 2.3	22.2 ± 2.0†
HR, bpm	682 ± 22	628 ± 16	542 ± 23	554 ± 21
SBP, mmHg	100 ± 4	139 ± 3**		
DBP, mmHg	60 ± 6	79 ± 4*		
MBP, mmHg	71 ± 5	99 ± 4**		

Data are expressed as mean ± SEM; n = 6 each; $^{*}P < 0.05$ and $^{**}P < 0.01$ compared with saline infused mice; $^{\dagger}P < 0.01$ compared with sham mice.
Ang II, angiotensin II; DBP, diastolic blood pressure; FS, fractional shortening; HR, heart rate; IVSD, interventricular septum diameter; LVEDD, left ventricular end-diastolic diameter; LVESD, left ventricular end-systolic diameter; LVPWD, left ventricular posterior wall diameter; MBP, mean blood pressure; SBP, systolic blood pressure; TAC, transverse aortic constriction.

Modulation of miR-21 altered PDCD4 expression *in vivo*

MiR-21 has been implicated in fibrosis by suppressing its downstream genes, such as

PDCD4, smad family member 7 (Smad7), phosphatase and tensin homolog (PTEN), and sprouty 1 (Spry1) [12, 15, 26, 27]. We examined the mRNA expression levels of these targets using qRT-PCR in Ang II infused mice and TAC mice hearts. PDCD4 mRNA levels were significantly downregulated in Ang II infused mice hearts compared with sham mice. PDCD4 mRNA levels were significantly lower in TAC mice hearts than in sham mice (Fig. 3A). Smad7 mRNA levels were significantly decreased in Ang II infused mice compared with sham mice, although there were no significant differences in PTEN and Spry1 mRNA levels between Ang II infused mice and sham mice (S1A Fig). There were no significant differences in Smad7, PTEN, and Spry1 mRNA levels between TAC mice and sham mice (S1B Fig).

Since PDCD4 mRNA levels were consistently decreased in Ang II infused mice and TAC mice hearts, we focused on PDCD4. We next investigated PDCD4 downstream target of transcription activator protein 1 (AP-1), a dimeric complex composed of c-Jun and c-Fos family, and TGF-β1 signaling pathway. AP-1 and TGF-β1 mRNA levels were significantly upregulated in Ang II infused mice hearts compared with those of saline infused mice (Fig. 3B). PDCD4 protein expression was significantly decreased in Ang II infused mice hearts, whereas c-Jun and TGF-β1 protein levels were significantly increased compared with those of saline infused mice

(Fig. 3C). AP-1 and TGF-β1 mRNA levels were significantly increased in the hearts of TAC mice compared with those of sham mice (Fig. 3D). Moreover, PDCD4 protein expression was significantly decreased in TAC mice hearts, whereas c-Jun and TGF-β1 protein levels were significantly increased compared with those of sham mice (Fig. 3E).

Fig 3. PDCD4 expression and its downstream signaling in Ang II- and TAC-induced cardiac remodeling.

(A) PDCD4 mRNA expression in Ang II infused and TAC-operated mice (n = 6 per group). **(B)** AP-1 and TGF-β1 mRNA expressions in Ang II infused mice (n = 6 per group). **(C)** Protein expressions of PDCD4, c-Jun, and TGF-β1 in Ang II infused mice (n = 6 per group). **(D)** AP-1 and TGF-β1 mRNA expressions in TAC-operated mice (n = 6 per group). **(E)** Protein expressions of PDCD4, c-Jun, and TGF-β1 in TAC-operated mice (n = 6 per group). Representative images from at least six independent results are shown. Data are expressed as mean ± SEM. $^{*}P < 0.05$.

The impact of miR-21 in cardiomyocytes under hypertrophic stimulation *in vitro*

MiR-21 expression levels were significantly increased in NRCMs under Ang II

297 stimulation (Fig. 4A). PDCD4 mRNA expression was significantly downregulated in
298 NRCMs under Ang II stimulation (Fig. 4B). However, there were no significant
299 differences in mRNA expression levels of Smad7, PTEN, and Spry1 in NRCMs (S2A
300 Fig). The mRNA expression levels of PDCD4, Smad7, and Spry1 were significantly
301 decreased in neonatal rat cardiofibroblasts under Ang II stimulation (S2B Fig). AP-1
302 and TGF-β1 mRNA levels were significantly upregulated in NRCMs under Ang II
303 stimulation (Fig. 4B). PDCD4 protein expressions were significantly decreased in
304 NRCMs under Ang II stimulation, whereas its targets, c-Jun and TGF-β1 protein
305 expression levels were significantly increased (Fig. 4C).
306 To verify whether PDCD4 directly interacts with AP-1 and subsequent
307 downregulation of TGF-β1, we transfected siPDCD4 into NRCMs. PDCD4 knockdown
308 significantly increased AP-1 and TGF-β1 mRNA levels (Fig. 4D). Western blot analysis
309 also revealed that c-Jun and TGF-β1 protein expression levels were significantly
310 increased by knockdown of PDCD4 (Fig. 4E).
311
312 **Fig 4. MiR-21 and PDCD4 expressions in cardiomyocytes under Ang II**
313 **stimulation.**
314 **(A)** MiR-21 expressions in cardiomyocytes under Ang II stimulation for 24 h (n = 4–6

315 per group). **(B)** PDCD4, AP-1, and TGF-β1 mRNA expressions in cardiomyocytes
316 under Ang II stimulation for 24 h (n = 4–6 per group). **(C)** Protein expression levels of
317 PDCD4, c-Jun, and TGF-β1 in cardiomyocytes under Ang II stimulation for 24 h (n =
318 4–6 per group). **(D)** AP-1 and TGF-β1 mRNA expressions in cardiomyocytes
319 transfected with siPDCD4 (n = 4–6 per group). **(E)** Protein expressions of PDCD4, c-
320 Jun, and TGF-β1 in cardiomyocytes transfected with siPDCD4 (n = 4–6 per group).
321 Representative images from at least four independent results are shown. Data are
322 expressed as mean ± SEM. **P* < 0.05.
323
324 To clarify the direct role of miR-21 in regulating PDCD4 expressions in NRCMs,
325 we transfected mirVana-miR-21-specific inhibitor into NRCMs. MiR-21 inhibitor
326 significantly upregulated PDCD4 mRNA expressions compared with negative control
327 (Fig. 5A). AP-1 and TGF-β1 mRNA expressions were significantly downregulated in
328 NRCMs with miR-21 inhibitor compared with those in the negative control. PDCD4
329 protein expression levels were significantly increased in NRCMs with miR-21 inhibitor
330 compared with those in the negative control, whereas its targets, c-Jun and TGF-β1
331 protein expression levels were significantly decreased under miR-21 inhibitor
332 transfection (Fig. 5B).

Fig 5. The impact of miR-21 suppression on PDCD4, AP-1, and TGF-β1 signaling in cardiomyocytes.

(A) Effect of miR-21 suppression on PDCD4, AP-1, and TGF-β1 mRNA expressions in cardiomyocytes (n = 4–6 per group). **(B)** Effect of miR-21 suppression on PDCD4, c-Jun, and TGF-β1 protein expressions in cardiomyocytes (n = 4–6 per group). Representative images from at least four independent results are shown. Data are expressed as mean ± SEM. **P* < 0.05.

MiR-21 inhibitor attenuated Ang II-induced PDCD4 suppression (Fig. 6A). As a result, subsequent Ang II-induced activation of AP-1 and TGF-β1 mRNA expressions were significantly suppressed by miR-21 inhibitor. PDCD4 protein expression levels were restored by inhibiting miR-21 expressions, whereas c-Jun and TGF-β1 protein expression levels were significantly suppressed (Fig. 6B).

MiR-21 inhibitor significantly suppressed the phosphorylation of TAK1, a key molecular for cardiac hypertrophy, in NRCMs under Ang II stimulation (Fig. 6C). Atrial natriuretic peptide (ANP) and brain natriuretic peptide (BNP) mRNA expressions were significantly upregulated in NRCMs under Ang II stimulation. MiR-21 inhibitor

significantly suppressed the mRNA expression of ANP and BNP in NRCMs under Ang II stimulation (Fig. 6D).

Fig 6. The impact of miR-21 suppression on cardiac remodeling under Ang II stimulation.

(A) Effect of miR-21 suppression on PDCD4, AP-1, and TGF-β1 mRNA expressions in cardiomyocytes under Ang II stimulation for 24 h (n = 4–6 per group). **(B)** Effect of miR-21 suppression on PDCD4, c-Jun, and TGF-β1 protein expressions in cardiomyocytes under Ang II stimulation for 24 h (n = 4–6 per group). **(C)** Effect of miR-21 suppression on TAK1 and pTAK1 expressions in cardiomyocytes under Ang II stimulation for 24 h (n = 4–6 per group). **(D)** Effect of miR-21 suppression on fetal gene expressions in cardiomyocytes under Ang II stimulation for 24 h (n = 4–6 per group). Representative images from at least four independent results are shown. Data are expressed as mean ± SEM. $^{*}P < 0.05$.

Discussion

In the present study, we revealed the functional role of miR-21 in hypertrophic cardiac remodeling. In patients with HHD, miR-21 expression levels were upregulated in the heart and blood samples. Furthermore, circulating miR-21 levels were positively correlated with serum markers of myocardial fibrosis. In cardiomyocytes, PDCD4 played a pivotal role in regulating cardiac remodeling as a target gene of miR-21 under hypertrophic stimulation. Knockdown of miR-21 ameliorated AP-1 mediated TGF-β1 signaling through regulating PDCD4 in cardiomyocytes. To the best of our knowledge, this study is the first report to evaluate the impact of miR-21 in patients with HHD, and that in cardiomyocytes in hypertrophic cardiac remodeling using *in vivo* and *in vitro* experiments. A schema that includes the suggested pathway from the present study is shown in Fig. 7.

Fig 7. A schema that includes the proposed pathway of miR-21 in cardiac remodeling

The pathogenetic mechanism of HHD is thought to be related to cardiac remodeling, including cardiac fibrosis and hypertrophy [28]. Hence, regression of

383 hypertrophic cardiac remodeling can improve the prognosis of patients with
384 hypertension. The contribution of miRs in the cardiomyopathies such as ischemic heart
385 disease, hypertrophic cardiomyopathy, and dilated cardiomyopathy has been shown [29-
386 31]. However, the impact of miR-21 as well as other miRs on the pathogenesis of HHD,
387 which is one of the most important hypertension-induced organ damages is still unclear.
388 In the present study, we showed that miR-21 expression levels were significantly
389 increased in both serum and heart samples of patients with HHD compared with normal
390 subjects. Moreover, there were significant positive correlations between circulating
391 miR-21 levels and serum markers of myocardial fibrosis. These findings support the
392 association between miR-21 and cardiac remodeling in patients with HHD.
393 It is well known that hypertension-derived mechanical stress induces Ang II
394 synthesis, and subsequent activation of nuclear AP-1 leads to the upregulation of TGF-
395 β1 [32]. TGF-β1 induces fibroblast-to-myofibroblast differentiation and extracellular
396 matrix (ECM) production, which leads to cardiac fibrosis [33]. It was reported that
397 TGF-β1 was increased with advancing of fibrosis in the hearts of patients who
398 underwent cardiac surgery [34]. While mice with systemic overexpression of TGF-β1
399 showed cardiac fibrosis and hypertrophy, mice with systemic knock-out of TGF-β1
400 ameliorated Ang II-induced cardiac hypertrophy [35, 36]. TGF-β1 is a key mediator of

401 the pathogenesis of cardiac remodeling under hypertrophic stimulation. Interestingly,
402 activation of TGF-β1 signaling increases miR-21 expressions [13]. In contrast, several
403 reports revealed that miR-21 can activate TGF-β1 signaling [11, 12]. This
404 interrelationship forms interesting positive feedback loop. Our results *in vivo* study
405 showed that miR-21 and TGF-β1 expression levels were significantly increased in Ang
406 II infused mice and TAC mice, suggesting that an interrelationship between miR-21 and
407 TGF-β1 may play an important role in hypertrophic cardiac remodeling.
408 Elevated miR-21 expression levels were reported to be associated with organ
409 fibrosis, such as lung, kidney, liver, and heart via promoting fibroblast activation [12,
410 16, 37, 38]. Several reports have shown the fibrogenic function of miR-21 in fibroblasts
411 through modulation of its target genes, such as PDCD4, Smad7, PTEN, and Spry1 [12,
412 15, 26, 27]. Thus, although the functional role of miR-21 in fibroblast is well known,
413 there were few studies assessing the functional role of miR-21 in cardiomyocyte. In the
414 present study, we found that Ang II significantly upregulated PDCD4 mRNA
415 expression in cardiomyocytes, although there were no significant differences in the
416 mRNA expression levels of Smad7, PTEN, and Spry1. These results suggest that
417 PDCD4 plays an important role in regulating cardiac remodeling as a target gene of
418 miR-21 under hypertrophic stimulation in cardiomyocyte.

PDCD4 is a well-known tumor suppressor and is involved in apoptosis. It was reported to be a powerful inhibitor of AP-1 [39]. On the other hand, activation of AP-1 upregulates miR-21 expressions [40]. In the present study, we showed that PDCD4 was significantly decreased and AP-1 was increased in Ang II infused mice and TAC mice. In addition, AP-1 mediated TGF-β1 expression was significantly upregulated under Ang II stimulation *in vitro*. Thus, there arises a possibility that miR-21 might enhance its own transcription through miR-21/PDCD4/AP-1 pathway and exacerbate the fibrogenic process in hypertrophic cardiac remodeling.

Cardiomyocytes and fibroblasts cooperatively regulate cardiac cell signaling via paracrine mediators, which is involved in cardiac remodeling [41]. It has been reported that TGF-β1 was induced in response to hypertrophic stimuli not only in fibroblasts but also in cardiomyocytes, and acting in a paracrine and/or autocrine manner [42, 43]. However, although the effects of miR-21 inhibition on cardiac remodeling were demonstrated in fibroblast, its effects in cardiomyocyte were poorly understood. In the present study, knockdown of miR-21 expression rescued Ang II-induced PDCD4 suppression. Furthermore, knockdown of miR-21 significantly suppressed Ang II-induced AP-1 and TGF-β1 signaling in cardiomyocytes. These results suggest that inhibition of miR-21 prevents hypertrophic stimulation-induced cardiac fibrosis by

437 suppressing miR-21/PDCD4/AP-1 feedback loop.

438 In addition to fibrogenic function of TGF-β1, Koitabashi et al. showed that
439 suppression of myocyte-derived TGF-β1 ameliorated cardiac hypertrophy by inhibiting
440 non-canonical pathways, in particular TAK1 [44]. Consistently, we showed that Ang II
441 stimulation induced TAK1 activation in cardiomyocytes. Furthermore, we showed that
442 inhibition of miR-21 expression suppressed TAK1 activity and subsequent fetal gene
443 expressions in cardiomyocytes. Remarkably, Thum et al. demonstrated that silencing of
444 miR-21 *in vivo* attenuated cardiac fibrosis and hypertrophy under pressure overload
445 stimulation through deactivation of cardiac fibroblast [15]. Taking our results into
446 consideration, this beneficial effect of miR-21 inhibitor in suppressing hypertrophic
447 cardiac remodeling might be attributed to not only cardiac fibroblast but also
448 cardiomyocyte.

449 We need to point out several limitations of our study. First, 3 patients with
450 hypertension were included in control group, although they had normal cardiac function
451 and had no left ventricular hypertrophy. Second, because there were 6 patients with
452 diabetes mellitus in HHD group, we could not completely rule out the possibility of the
453 influence of diabetes mellitus on cardiac remodeling. Third, EMB study size was
454 relatively small for investigating the impact of miR-21 on cardiac remodeling in

455 patients with HHD. Finally, we have not evaluated the effect of miR-21 inhibitor *in*

456 *vivo*. Several studies demonstrated that inhibition of miR-21 suppressed cardiac

457 remodeling by regulating cardiac fibroblast [15, 16, 26], although we confirmed the

458 protective effect of miR-21 inhibitor in cardiomyocyte under hypertrophic stimulation

459 *in vitro*.

Conclusions

MiR-21 was associated with fibrogenesis in heart under hypertrophic stimulation.

Inhibition of miR-21 expressions prevent hypertrophic cardiac remodeling by regulating PDCD4 and AP-1, TGF-β1 signaling pathway.

464 # Acknowledgement

465 We thank Ms. Emiko Nishidate and Ms. Hiroko Sasaki for their excellent technical

466 assistance and comments.

References

1. Worldwide trends in blood pressure from 1975 to 2015: a pooled analysis of 1479 population-based measurement studies with 19.1 million participants. Lancet (London, England). 2017;389(10064):37-55. Epub 2016/11/20. doi: 10.1016/s0140-6736(16)31919-5. PubMed PMID: 27863813; PubMed Central PMCID: PMCPMC5220163.

2. Mills KT, Bundy JD, Kelly TN, Reed JE, Kearney PM, Reynolds K, et al. Global Disparities of Hypertension Prevalence and Control: A Systematic Analysis of Population-Based Studies From 90 Countries. Circulation. 2016;134(6):441-50. Epub 2016/08/10. doi: 10.1161/circulationaha.115.018912. PubMed PMID: 27502908; PubMed Central PMCID: PMCPMC4979614.

3. Williams B, Mancia G, Spiering W, Agabiti Rosei E, Azizi M, Burnier M, et al. 2018 ESC/ESH Guidelines for the management of arterial hypertension. Eur Heart J. 2018;39(33):3021-104. Epub 2018/08/31. doi: 10.1093/eurheartj/ehy339. PubMed PMID: 30165516.

4. Drazner MH. The progression of hypertensive heart disease. Circulation. 2011;123(3):327-34. Epub 2011/01/26. doi: 10.1161/circulationaha.108.845792. PubMed PMID: 21263005.

5. Haider AW, Larson MG, Franklin SS, Levy D. Systolic blood pressure, diastolic blood pressure, and pulse pressure as predictors of risk for congestive heart failure in the Framingham Heart Study. Annals of internal medicine. 2003;138(1):10-6. Epub 2003/01/07. PubMed PMID: 12513039.

6. Runte KE, Bell SP, Selby DE, Haussler TN, Ashikaga T, LeWinter MM, et al. Relaxation and the Role of Calcium in Isolated Contracting Myocardium From Patients With Hypertensive Heart Disease and Heart Failure With Preserved Ejection Fraction. Circulation Heart failure. 2017;10(8). Epub 2017/08/09. doi: 10.1161/circheartfailure.117.004311. PubMed PMID: 28784688; PubMed Central PMCID: PMCPMC5567852.

7. Owan TE, Hodge DO, Herges RM, Jacobsen SJ, Roger VL, Redfield MM. Trends in prevalence and outcome of heart failure with preserved ejection fraction. The New England journal of medicine. 2006;355(3):251-9. Epub 2006/07/21. doi: 10.1056/NEJMoa052256. PubMed PMID: 16855265.

8. Jiang X, Tsitsiou E, Herrick SE, Lindsay MA. MicroRNAs and the regulation of fibrosis. The FEBS journal. 2010;277(9):2015-21. Epub 2010/04/24. doi: 10.1111/j.1742-4658.2010.07632.x. PubMed PMID: 20412055; PubMed Central PMCID: PMCPMC2963651.

9. Huang Y, He Y, Li J. MicroRNA-21: a central regulator of fibrotic diseases via various targets. Curr Pharm Des. 2015;21(17):2236-42. Epub 2014/12/30. doi: 10.2174/1381612820666141226095701. PubMed PMID: 25541205.

10. Dobaczewski M, Chen W, Frangogiannis NG. Transforming growth factor (TGF)-beta signaling in cardiac remodeling. Journal of molecular and cellular cardiology. 2011;51(4):600-6. Epub 2010/11/10. doi: 10.1016/j.yjmcc.2010.10.033. PubMed PMID: 21059352; PubMed Central PMCID: PMCPMC3072437.

11. Liu RH, Ning B, Ma XE, Gong WM, Jia TH. Regulatory roles of microRNA-21 in fibrosis through interaction with diverse pathways (Review). Molecular medicine reports. 2016;13(3):2359-66. Epub 2016/02/06. doi: 10.3892/mmr.2016.4834. PubMed PMID: 26846276.

12. Sun Q, Miao J, Luo J, Yuan Q, Cao H, Su W, et al. The feedback loop between miR-21, PDCD4 and AP-1 functions as a driving force for renal fibrogenesis. J Cell Sci. 2018;131(6). Epub 2018/01/24. doi: 10.1242/jcs.202317. PubMed PMID: 29361523.

13. Davis BN, Hilyard AC, Lagna G, Hata A. SMAD proteins control DROSHA-mediated microRNA maturation. Nature. 2008;454(7200):56-61. Epub 2008/06/13. doi: 10.1038/nature07086. PubMed PMID: 18548003; PubMed Central PMCID: PMCPMC2653422.

14. Fang L, Ellims AH, Moore XL, White DA, Taylor AJ, Chin-Dusting J, et al. Circulating microRNAs as biomarkers for diffuse myocardial fibrosis in patients with hypertrophic cardiomyopathy. Journal of translational medicine. 2015;13:314. Epub 2015/09/26. doi: 10.1186/s12967-015-0672-0. PubMed PMID: 26404540; PubMed Central PMCID: PMCPMC4581079.

15. Thum T, Gross C, Fiedler J, Fischer T, Kissler S, Bussen M, et al. MicroRNA-21 contributes to myocardial disease by stimulating MAP kinase signalling in fibroblasts. Nature. 2008;456(7224):980-4. Epub 2008/12/02. doi: 10.1038/nature07511. PubMed PMID: 19043405.

16. Lorenzen JM, Schauerte C, Hubner A, Kolling M, Martino F, Scherf K, et al. Osteopontin is indispensible for AP1-mediated angiotensin II-related miR-21 transcription during cardiac fibrosis. Eur Heart J. 2015;36(32):2184-96. Epub 2015/04/23. doi: 10.1093/eurheartj/ehv109. PubMed PMID: 25898844; PubMed Central PMCID: PMCPMC4543785.

17. Kitahara T, Takeishi Y, Arimoto T, Niizeki T, Koyama Y, Sasaki T, et al. Serum carboxy-terminal telopeptide of type I collagen (ICTP) predicts cardiac events in chronic heart failure patients with preserved left ventricular systolic function. Circulation journal : official journal of the Japanese Circulation Society. 2007;71(6):929-35. Epub 2007/05/29. PubMed PMID: 17526992.

18. Takahashi T, Shishido T, Kinoshita D, Watanabe K, Toshima T, Sugai T, et al. Cardiac Nuclear High-Mobility Group Box 1 Ameliorates Pathological Cardiac Hypertrophy by Inhibiting DNA Damage Response. JACC Basic to translational science. 2019;4(2):234-47. Epub

538 2019/05/08. doi: 10.1016/j.jacbts.2018.11.011. PubMed PMID: 31061925; PubMed Central
539 PMCID: PMCPMC6488753.
540 19. Carnevale D, Mascio G, D'Andrea I, Fardella V, Bell RD, Branchi I, et al. Hypertension
541 induces brain beta-amyloid accumulation, cognitive impairment, and memory deterioration
542 through activation of receptor for advanced glycation end products in brain vasculature.
543 Hypertension. 2012;60(1):188-97. Epub 2012/05/23. doi:
544 10.1161/hypertensionaha.112.195511. PubMed PMID: 22615109; PubMed Central PMCID:
545 PMCPMC3530195.
546 20. Netsu S, Shishido T, Kitahara T, Honda Y, Funayama A, Narumi T, et al. Midkine
547 exacerbates pressure overload-induced cardiac remodeling. Biochem Biophys Res Commun.
548 2014;443(1):205-10. Epub 2013/12/03. doi: 10.1016/j.bbrc.2013.11.083. PubMed PMID:
549 24291499.
550 21. Otaki Y, Takahashi H, Watanabe T, Funayama A, Netsu S, Honda Y, et al. HECT-Type
551 Ubiquitin E3 Ligase ITCH Interacts With Thioredoxin-Interacting Protein and Ameliorates
552 Reactive Oxygen Species-Induced Cardiotoxicity. J Am Heart Assoc. 2016;5(1). doi:
553 10.1161/JAHA.115.002485. PubMed PMID: 26796253; PubMed Central PMCID:
554 PMCPMC4859366.
555 22. Song J, Zhu Y, Li J, Liu J, Gao Y, Ha T, et al. Pellino1-mediated TGF-beta1 synthesis
556 contributes to mechanical stress induced cardiac fibroblast activation. Journal of molecular and
557 cellular cardiology. 2015;79:145-56. Epub 2014/12/03. doi: 10.1016/j.yjmcc.2014.11.006.
558 PubMed PMID: 25446187.
559 23. Takahashi H, Takeishi Y, Seidler T, Arimoto T, Akiyama H, Hozumi Y, et al. Adenovirus-
560 mediated overexpression of diacylglycerol kinase-zeta inhibits endothelin-1-induced
561 cardiomyocyte hypertrophy. Circulation. 2005;111(12):1510-6. Epub 2005/03/23. doi:
562 10.1161/01.Cir.0000159339.00703.22. PubMed PMID: 15781737.
563 24. van Rooij E, Olson EN. Searching for miR-acles in cardiac fibrosis. Circ Res.
564 2009;104(2):138-40. Epub 2009/01/31. doi: 10.1161/circresaha.108.192492. PubMed PMID:
565 19179664; PubMed Central PMCID: PMCPMC2747251.
566 25. Mansour IN, Bress AP, Groo V, Ismail S, Wu G, Patel SR, et al. Circulating Procollagen
567 Type III N-Terminal Peptide and Mortality Risk in African Americans With Heart Failure.
568 Journal of cardiac failure. 2016;22(9):692-9. Epub 2016/01/02. doi:
569 10.1016/j.cardfail.2015.12.016. PubMed PMID: 26721774; PubMed Central PMCID:
570 PMCPMC4917490.
571 26. Yuan J, Chen H, Ge D, Xu Y, Xu H, Yang Y, et al. Mir-21 Promotes Cardiac Fibrosis After
572 Myocardial Infarction Via Targeting Smad7. Cellular physiology and biochemistry : international
573 journal of experimental cellular physiology, biochemistry, and pharmacology. 2017;42(6):2207-

574 19. Epub 2017/08/18. doi: 10.1159/000479995. PubMed PMID: 28817807.
575 27. Roy S, Khanna S, Hussain SR, Biswas S, Azad A, Rink C, et al. MicroRNA expression in
576 response to murine myocardial infarction: miR-21 regulates fibroblast metalloprotease-2 via
577 phosphatase and tensin homologue. Cardiovasc Res. 2009;82(1):21-9. Epub 2009/01/17. doi:
578 10.1093/cvr/cvp015. PubMed PMID: 19147652; PubMed Central PMCID: PMCPMC2652741.
579 28. Weber KT, Sun Y, Gerling IC, Guntaka RV. Regression of Established Cardiac Fibrosis in
580 Hypertensive Heart Disease. American journal of hypertension. 2017;30(11):1049-52. Epub
581 2017/04/06. doi: 10.1093/ajh/hpx054. PubMed PMID: 28379281.
582 29. Li X, Yang Y, Wang L, Qiao S, Lu X, Wu Y, et al. Plasma miR-122 and miR-3149 Potentially
583 Novel Biomarkers for Acute Coronary Syndrome. PLoS One. 2015;10(5):e0125430. Epub
584 2015/05/02. doi: 10.1371/journal.pone.0125430. PubMed PMID: 25933289; PubMed Central
585 PMCID: PMCPMC4416808.
586 30. Kuster DW, Mulders J, Ten Cate FJ, Michels M, Dos Remedios CG, da Costa Martins PA,
587 et al. MicroRNA transcriptome profiling in cardiac tissue of hypertrophic cardiomyopathy
588 patients with MYBPC3 mutations. Journal of molecular and cellular cardiology. 2013;65:59-66.
589 Epub 2013/10/03. doi: 10.1016/j.yjmcc.2013.09.012. PubMed PMID: 24083979.
590 31. Zhou Q, Schotterl S, Backes D, Brunner E, Hahn JK, Ionesi E, et al. Inhibition of miR-208b
591 improves cardiac function in titin-based dilated cardiomyopathy. Int J Cardiol. 2017;230:634-41.
592 Epub 2017/01/10. doi: 10.1016/j.ijcard.2016.12.171. PubMed PMID: 28065693.
593 32. Rosenkranz S. TGF-beta1 and angiotensin networking in cardiac remodeling. Cardiovasc
594 Res. 2004;63(3):423-32. Epub 2004/07/28. doi: 10.1016/j.cardiores.2004.04.030. PubMed
595 PMID: 15276467.
596 33. Weber KT, Sun Y, Bhattacharya SK, Ahokas RA, Gerling IC. Myofibroblast-mediated
597 mechanisms of pathological remodelling of the heart. Nature reviews Cardiology. 2013;10(1):15-
598 26. Epub 2012/12/05. doi: 10.1038/nrcardio.2012.158. PubMed PMID: 23207731.
599 34. Hein S, Arnon E, Kostin S, Schonburg M, Elsasser A, Polyakova V, et al. Progression from
600 compensated hypertrophy to failure in the pressure-overloaded human heart: structural
601 deterioration and compensatory mechanisms. Circulation. 2003;107(7):984-91. Epub
602 2003/02/26. PubMed PMID: 12600911.
603 35. Rosenkranz S, Flesch M, Amann K, Haeuseler C, Kilter H, Seeland U, et al. Alterations of
604 beta-adrenergic signaling and cardiac hypertrophy in transgenic mice overexpressing TGF-
605 beta(1). American journal of physiology Heart and circulatory physiology. 2002;283(3):H1253-
606 62. Epub 2002/08/16. doi: 10.1152/ajpheart.00578.2001. PubMed PMID: 12181157.
607 36. Schultz Jel J, Witt SA, Glascock BJ, Nieman ML, Reiser PJ, Nix SL, et al. TGF-beta1
608 mediates the hypertrophic cardiomyocyte growth induced by angiotensin II. J Clin Invest.
609 2002;109(6):787-96. Epub 2002/03/20. doi: 10.1172/jci14190. PubMed PMID: 11901187;

610 PubMed Central PMCID: PMCPMC150912.
611 37. Sun NN, Yu CH, Pan MX, Zhang Y, Zheng BJ, Yang QJ, et al. Mir-21 Mediates the
612 Inhibitory Effect of Ang (1-7) on AngII-induced NLRP3 Inflammasome Activation by Targeting
613 Spry1 in lung fibroblasts. Scientific reports. 2017;7(1):14369. Epub 2017/11/01. doi:
614 10.1038/s41598-017-13305-3. PubMed PMID: 29084974; PubMed Central PMCID:
615 PMCPMC5662719.
616 38. Zhang Z, Zha Y, Hu W, Huang Z, Gao Z, Zang Y, et al. The autoregulatory feedback loop of
617 microRNA-21/programmed cell death protein 4/activation protein-1 (MiR-21/PDCD4/AP-1)
618 as a driving force for hepatic fibrosis development. J Biol Chem. 2013;288(52):37082-93. Epub
619 2013/11/08. doi: 10.1074/jbc.M113.517953. PubMed PMID: 24196965; PubMed Central
620 PMCID: PMCPMC3873564.
621 39. Yang HS, Knies JL, Stark C, Colburn NH. Pdcd4 suppresses tumor phenotype in JB6 cells
622 by inhibiting AP-1 transactivation. Oncogene. 2003;22(24):3712-20. Epub 2003/06/13. doi:
623 10.1038/sj.onc.1206433. PubMed PMID: 12802278.
624 40. Talotta F, Cimmino A, Matarazzo MR, Casalino L, De Vita G, D'Esposito M, et al. An
625 autoregulatory loop mediated by miR-21 and PDCD4 controls the AP-1 activity in RAS
626 transformation. Oncogene. 2009;28(1):73-84. Epub 2008/10/14. doi: 10.1038/onc.2008.370.
627 PubMed PMID: 18850008.
628 41. Pellman J, Zhang J, Sheikh F. Myocyte-fibroblast communication in cardiac fibrosis and
629 arrhythmias: Mechanisms and model systems. Journal of molecular and cellular cardiology.
630 2016;94:22-31. Epub 2016/03/22. doi: 10.1016/j.yjmcc.2016.03.005. PubMed PMID:
631 26996756; PubMed Central PMCID: PMCPMC4861678.
632 42. Takahashi N, Calderone A, Izzo NJ, Jr., Maki TM, Marsh JD, Colucci WS. Hypertrophic
633 stimuli induce transforming growth factor-beta 1 expression in rat ventricular myocytes. J Clin
634 Invest. 1994;94(4):1470-6. Epub 1994/10/01. doi: 10.1172/jci117485. PubMed PMID:
635 7929822; PubMed Central PMCID: PMCPMC295284.
636 43. Gray MO, Long CS, Kalinyak JE, Li HT, Karliner JS. Angiotensin II stimulates cardiac
637 myocyte hypertrophy via paracrine release of TGF-beta 1 and endothelin-1 from fibroblasts.
638 Cardiovasc Res. 1998;40(2):352-63. Epub 1999/01/20. doi: 10.1016/s0008-6363(98)00121-7.
639 PubMed PMID: 9893729.
640 44. Koitabashi N, Danner T, Zaiman AL, Pinto YM, Rowell J, Mankowski J, et al. Pivotal role of
641 cardiomyocyte TGF-beta signaling in the murine pathological response to sustained pressure
642 overload. J Clin Invest. 2011;121(6):2301-12. Epub 2011/05/04. doi: 10.1172/jci44824.
643 PubMed PMID: 21537080; PubMed Central PMCID: PMCPMC3104748.
644
645

Supporting information

S1 Fig. Smad7, PTEN, and Spry1 mRNA levels in Ang II infused and TAC mice.

(A) Smad7, PTEN, and Spry1 mRNA levels in Ang II infused mice compared with those of saline infused mice (n = 6 per group). **(B)** Smad7, PTEN, and Spry1 mRNA levels in TAC mice compared with those of sham mice (n = 6 per group). Data are expressed as mean ± SEM. **P* < 0.05.

S2 Fig. The differences in the expression levels of miR-21 targets between cardiomyocytes and cardiofibroblasts.

(A) The mRNA expressions of Smad7, PTEN, and Spry1 after treatment with vehicle or Ang II for 24 h in NRCMs (n = 4–6 per group). **(B)** The mRNA expressions of PDCD4, Smad7, PTEN, and Spry1 after treatment with vehicle or Ang II for 24 h in cardiofibroblasts (n = 4–6 per group). Data are expressed as mean ± SEM. **P* < 0.05.

Fig. 1

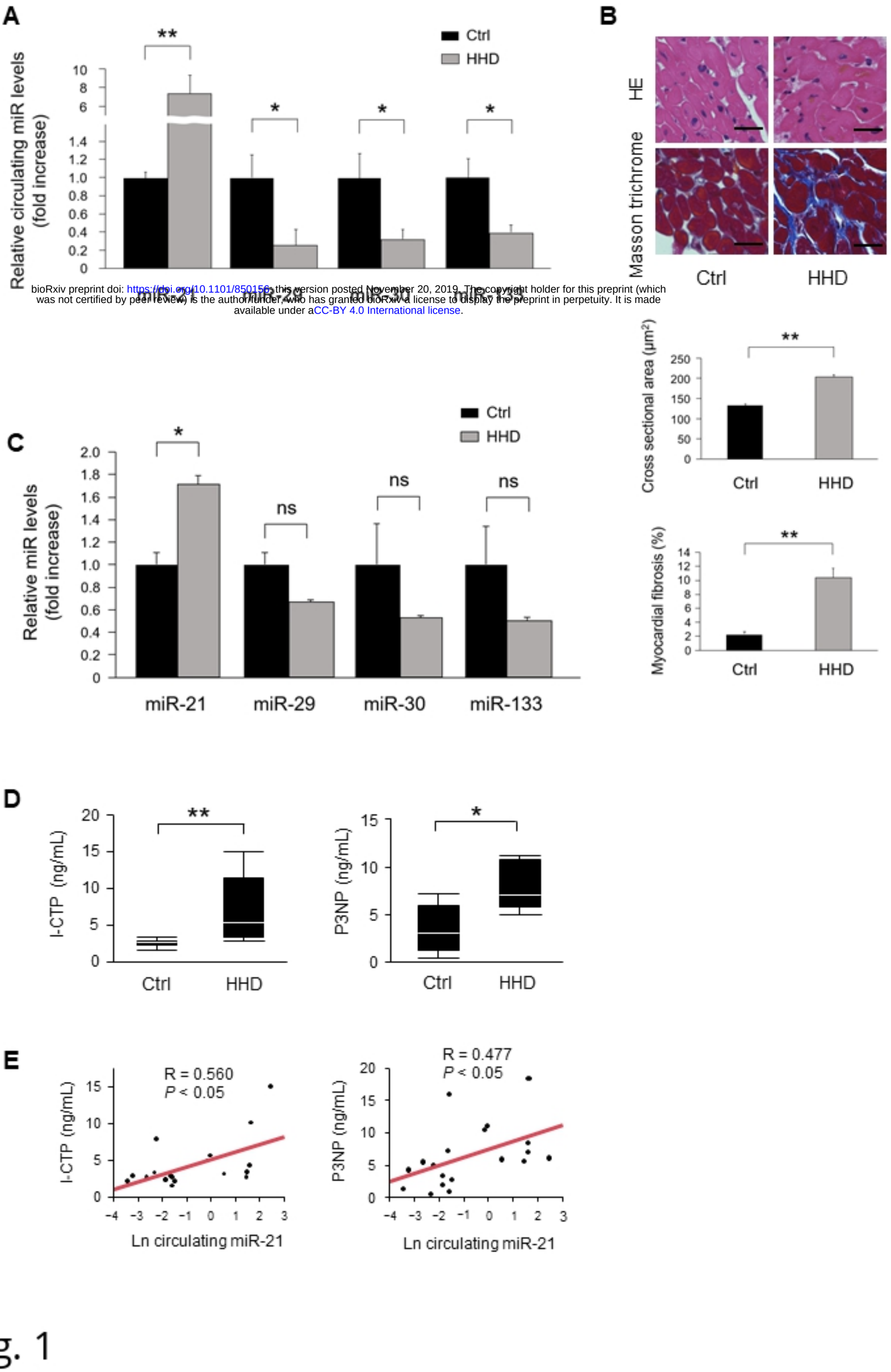

Fig. 1

Fig. 2

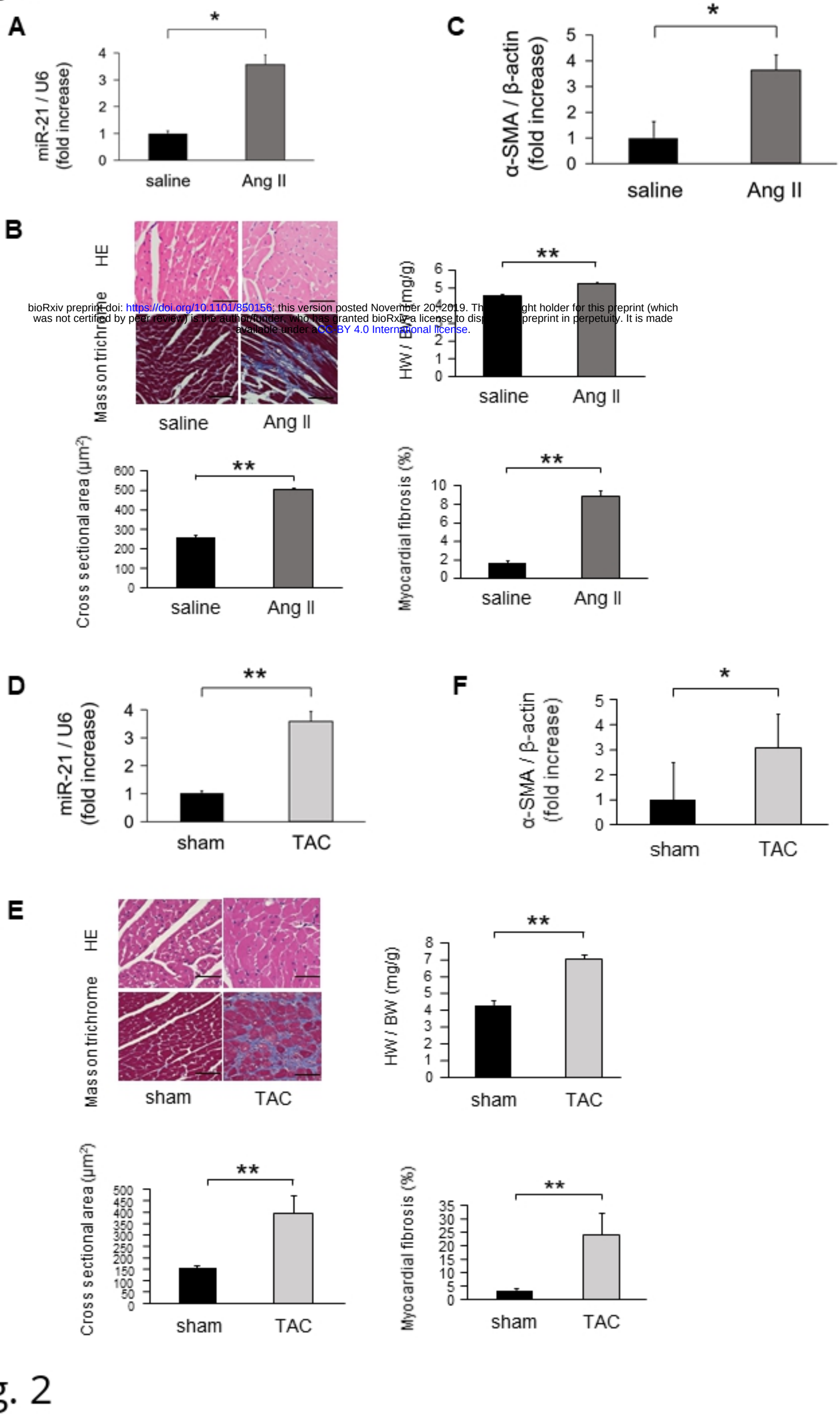

Fig. 2

Fig. 3

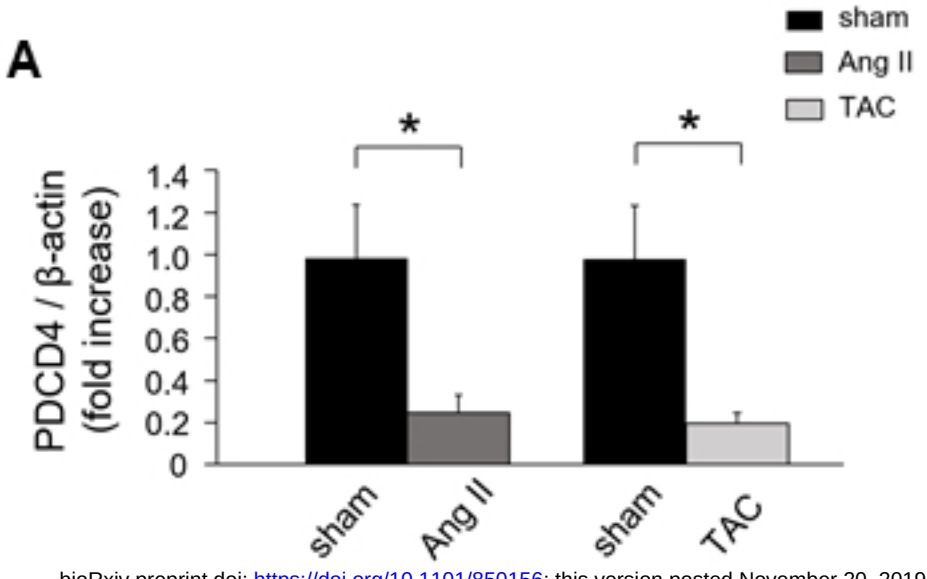

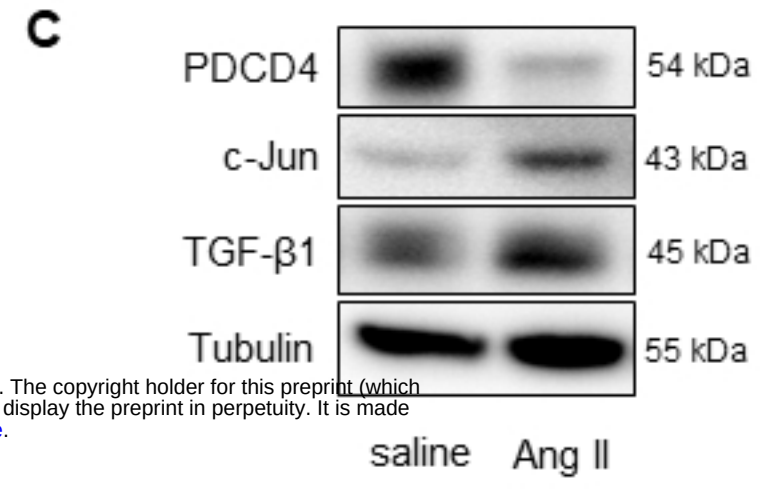

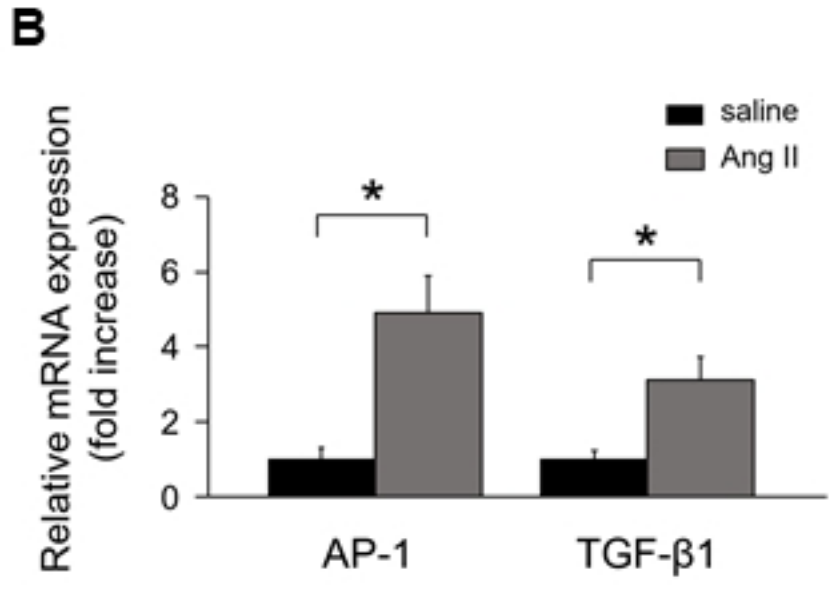

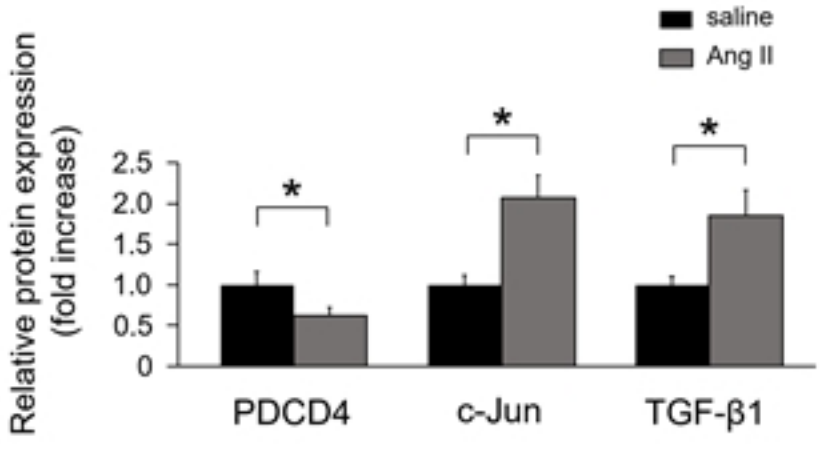

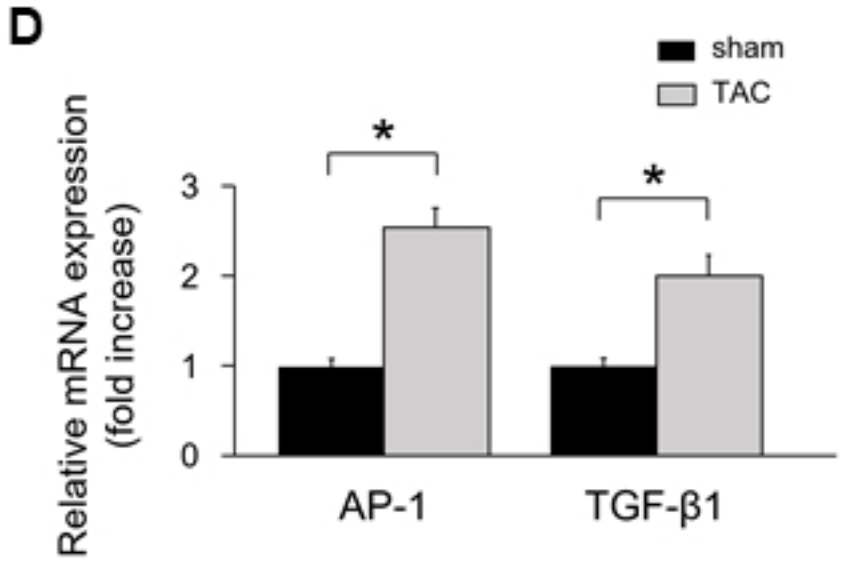

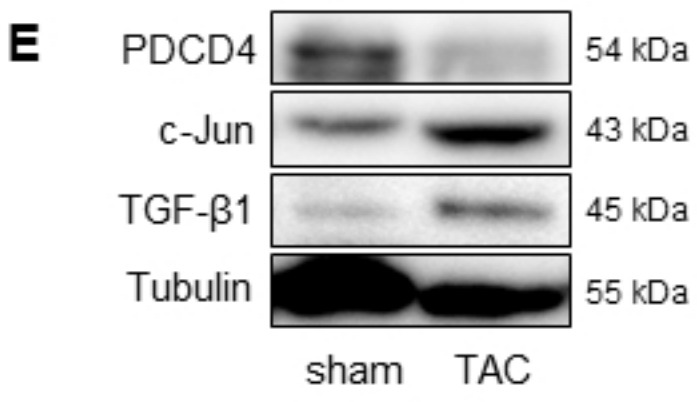

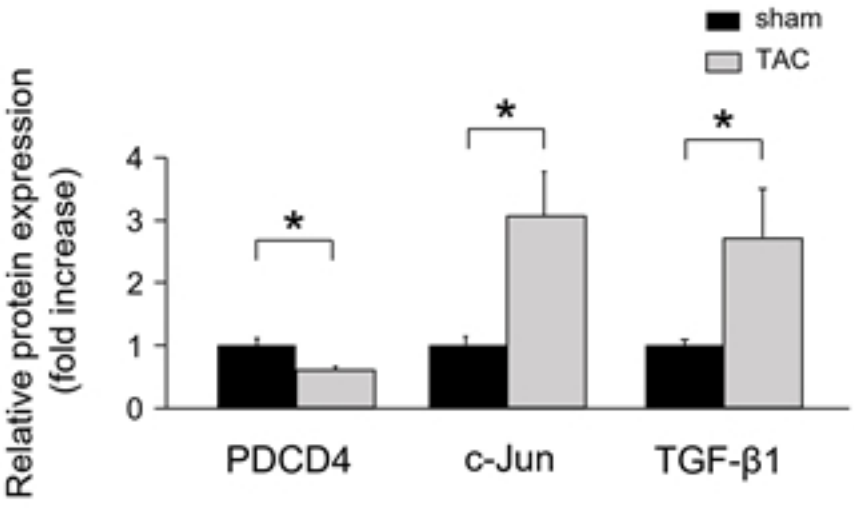

Fig. 3

Fig. 4

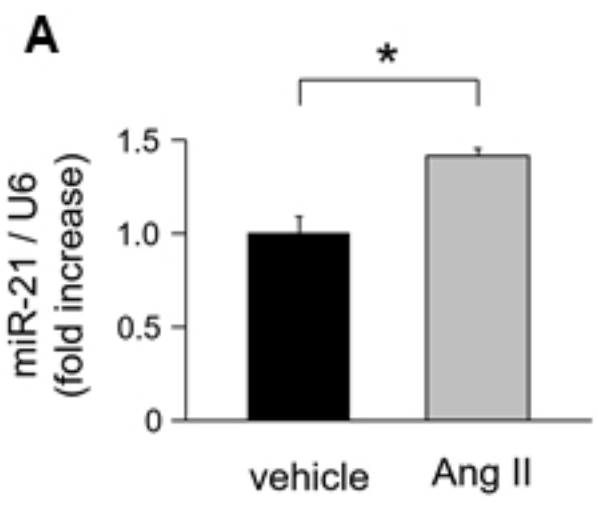

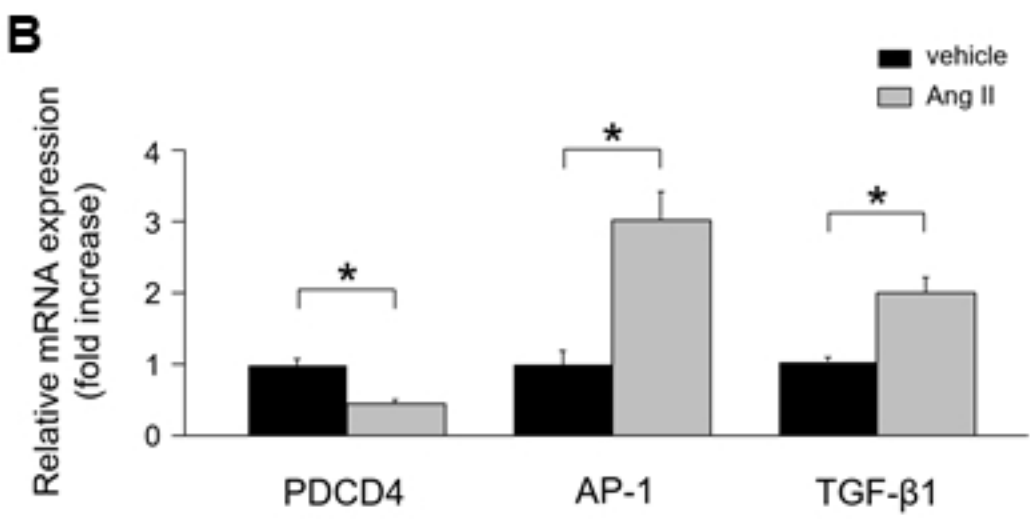

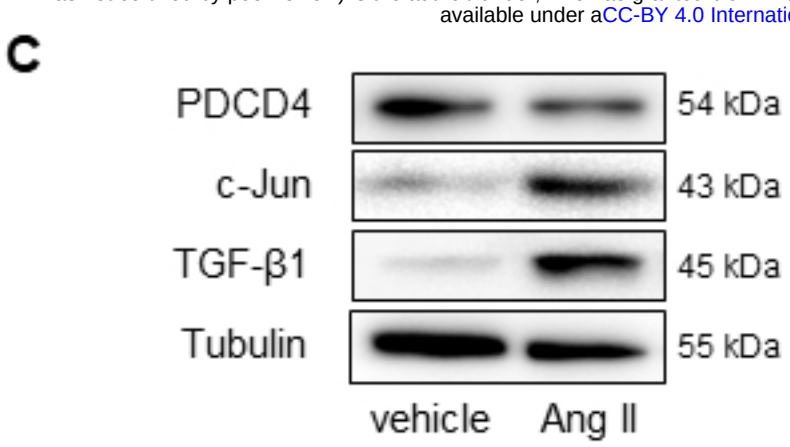

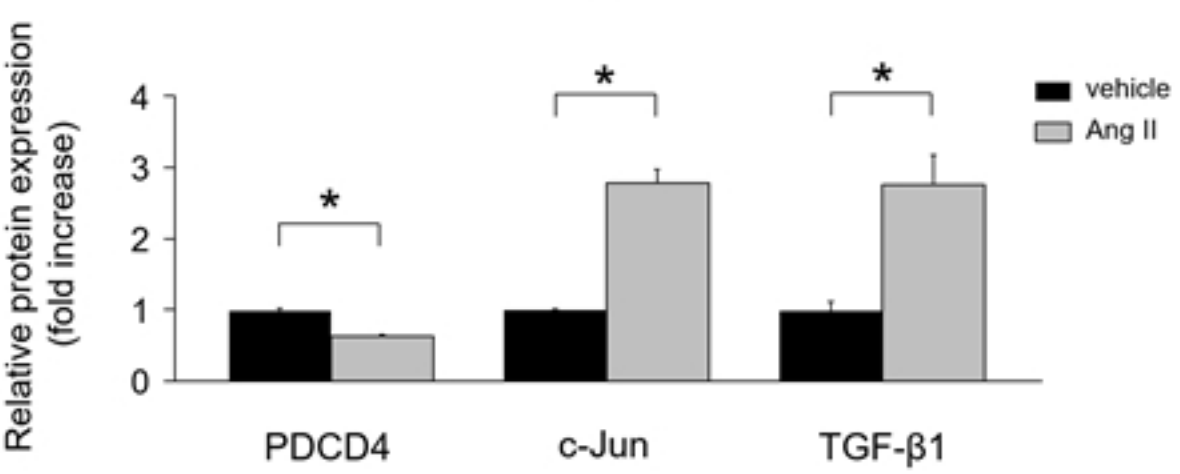

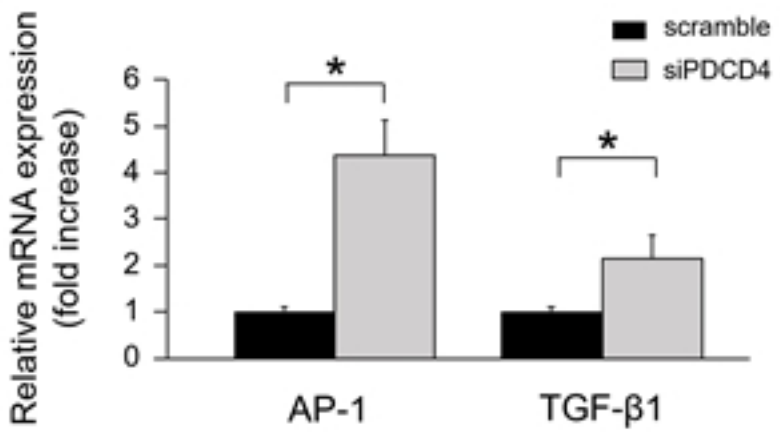

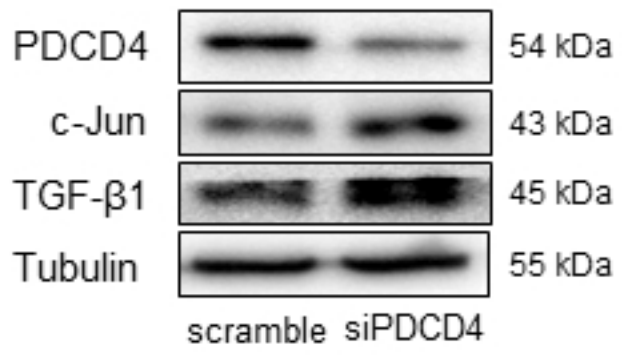

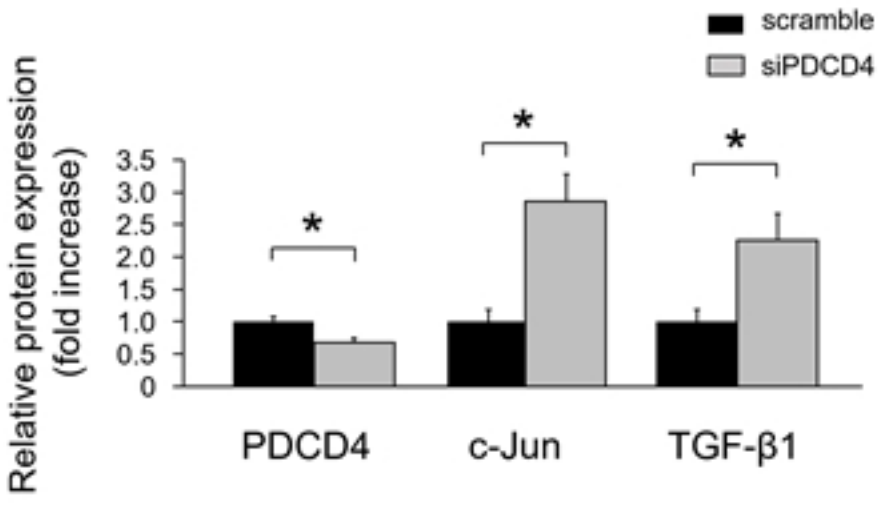

Fig. 4

Fig. 5

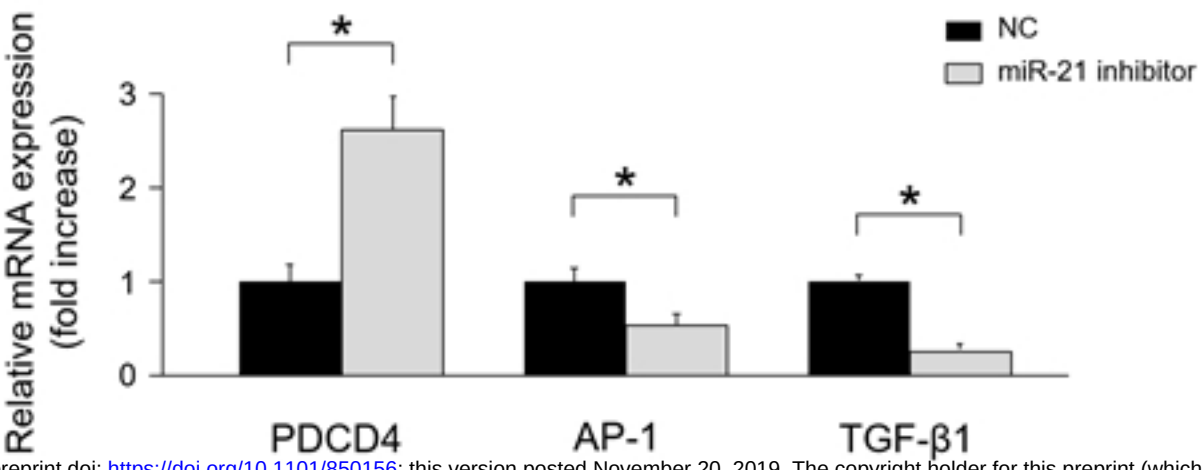

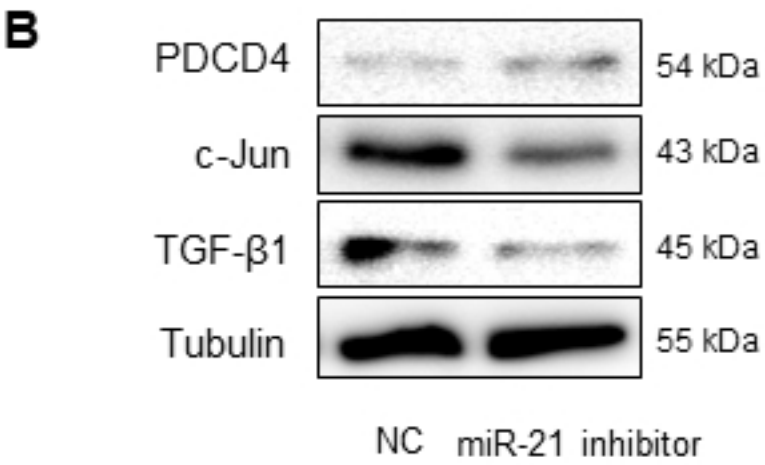

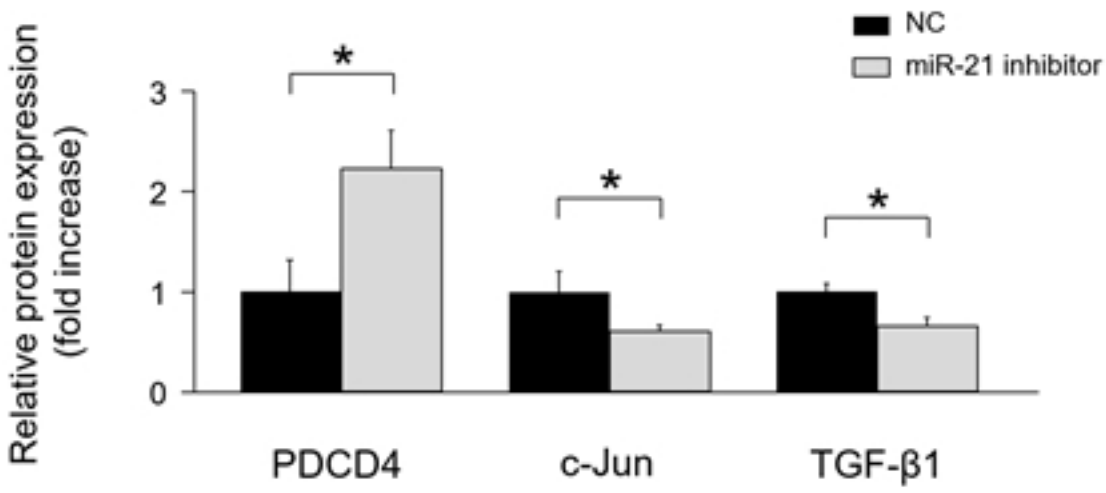

Fig. 5

Fig. 6

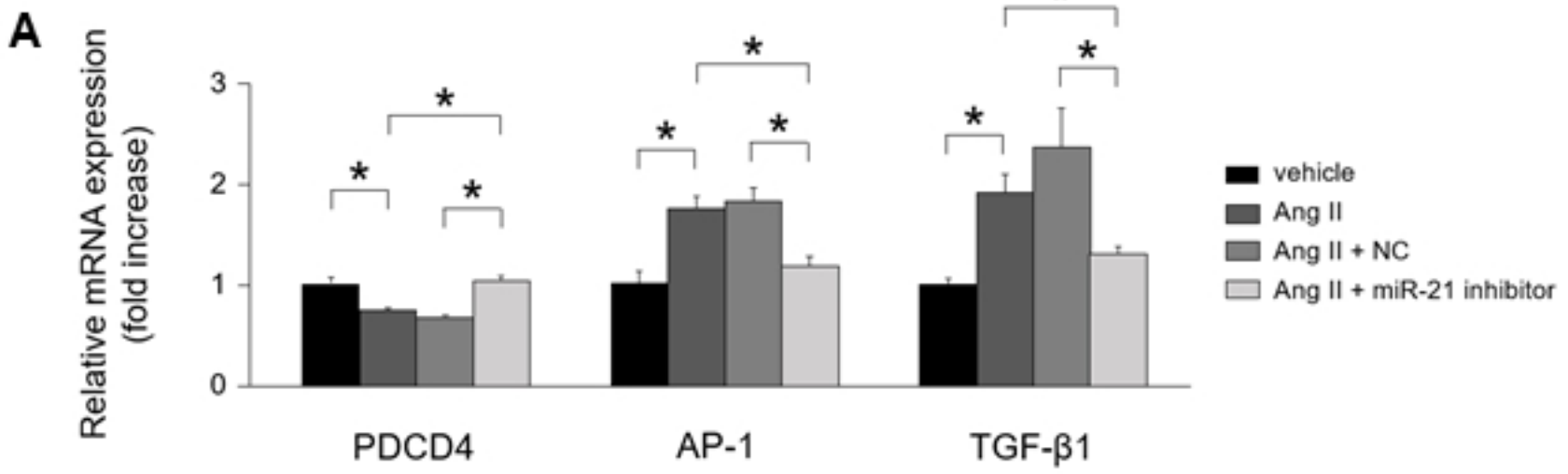

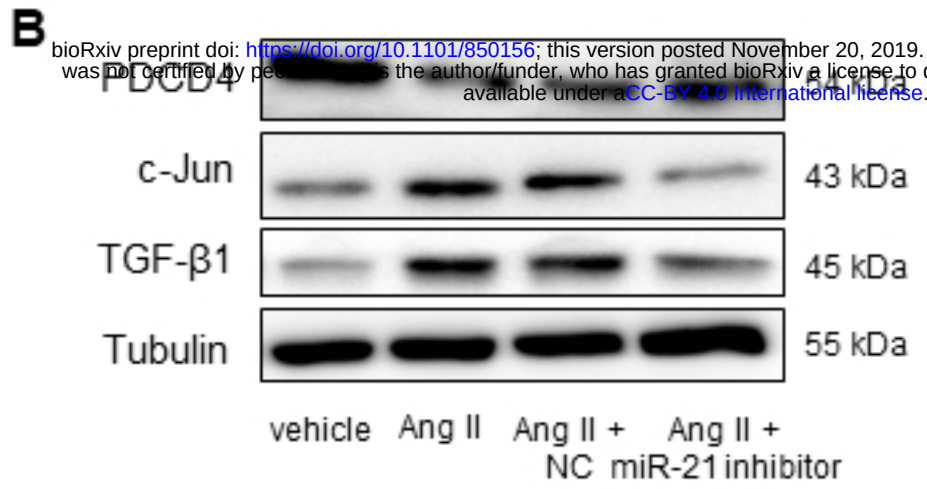

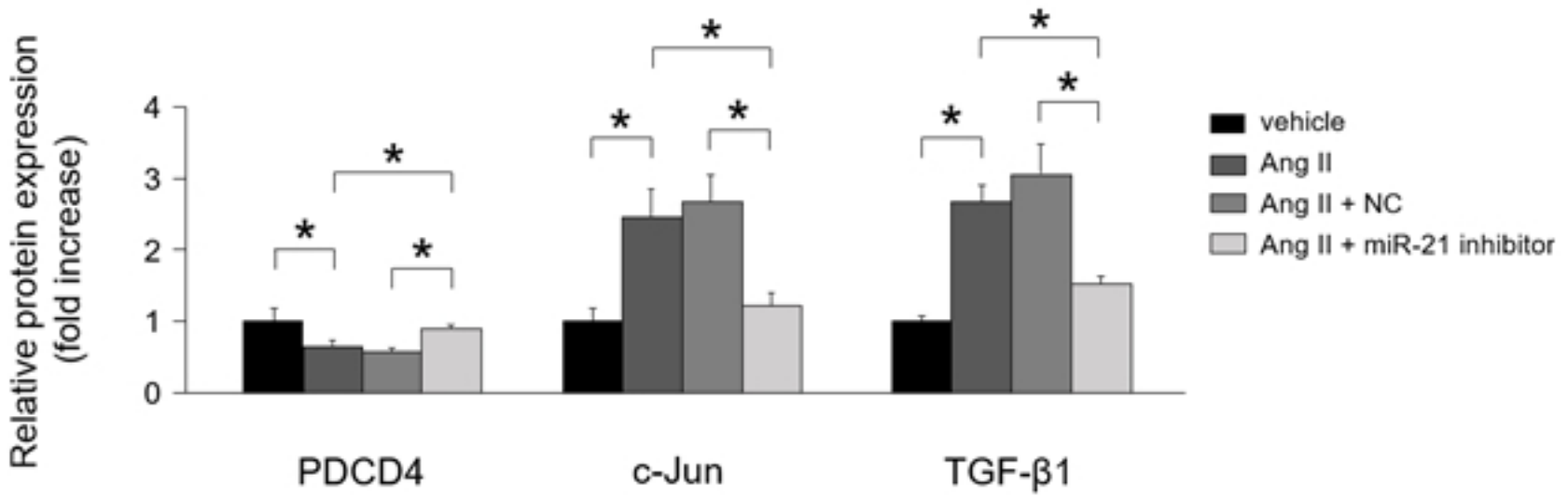

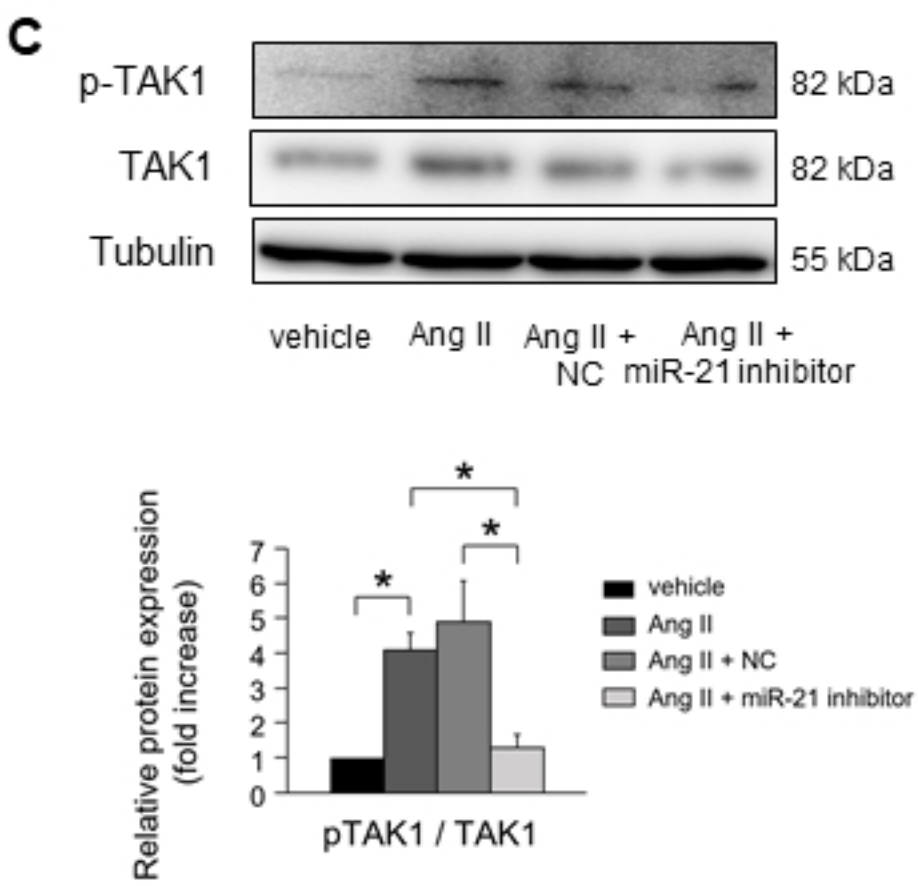

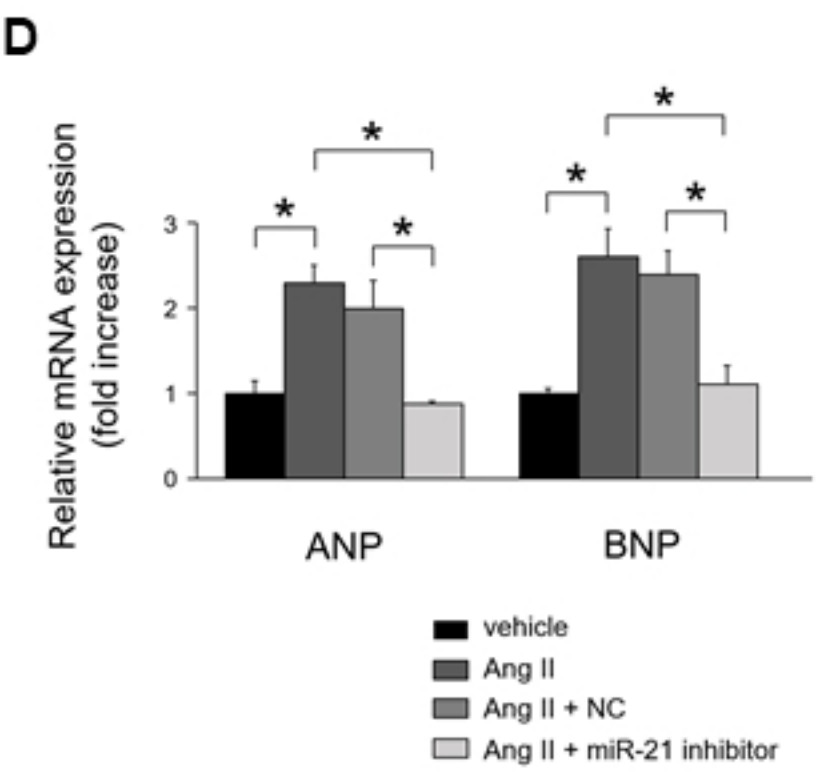

Fig. 6

Fig. 7

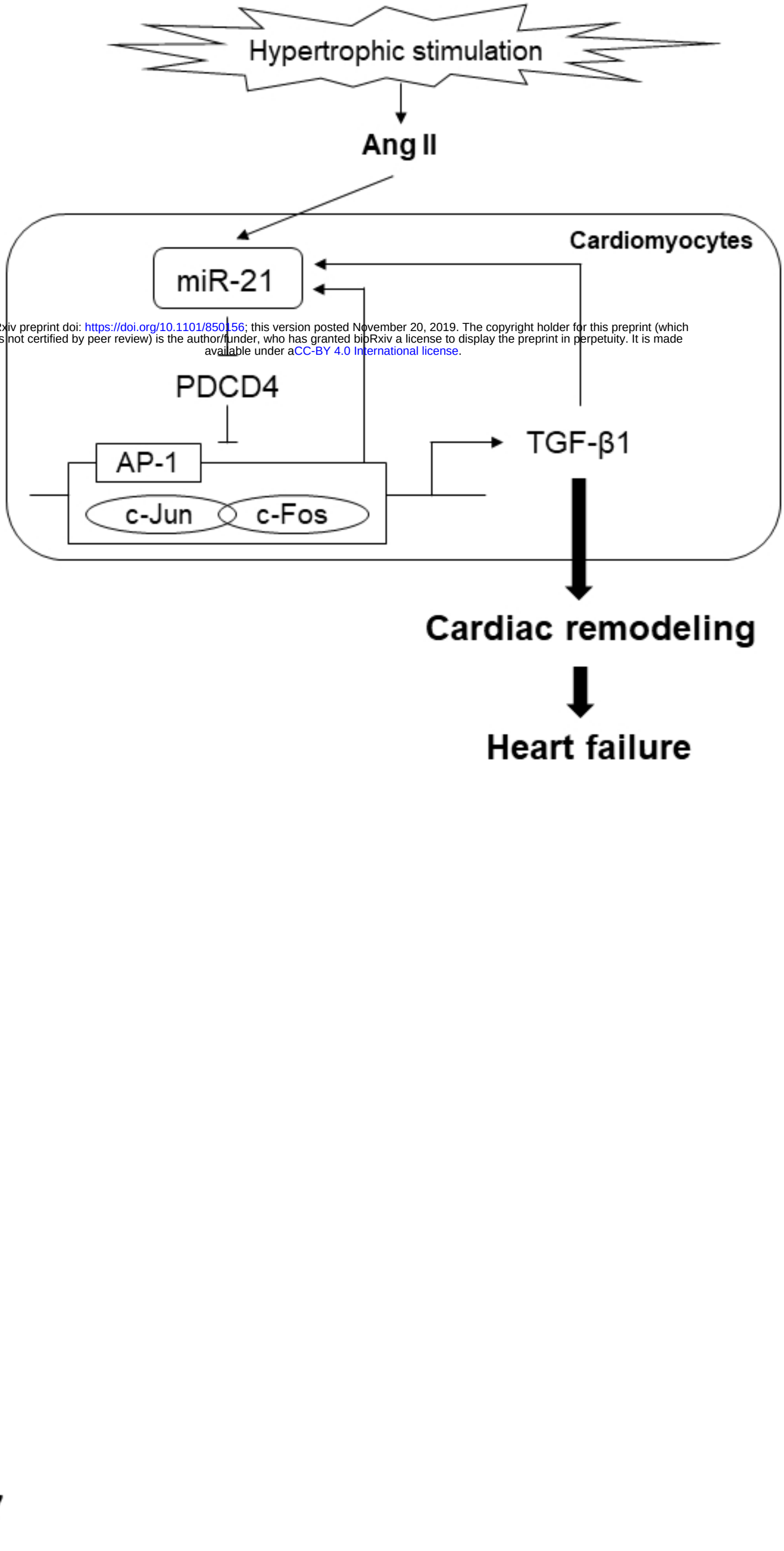

Fig. 7